XLIII CILAMCE
21–25, November, 2022
FOZ DO IGUAÇU – PR – BRAZIL

A Variational Full-Network Constitutive Model with Anisotropic Damage and Viscoelasticity Induced by Deformation for Biological Tissues

Daniel M. Cruz[1], Francisco L. Bresolin[1], Jakson M. Vassoler[1]

[1]*Department of Mechanical Engineering, Federal University of Rio Grande do Sul*
Rua Sarmento Leite, 425, Centro Histórico, Porto Alegre, 90050-170, Rio Grande do Sul, Brazil
daniel.cruz@ufrgs.br, francisco.bresolin@ufrgs.br, jmvassoler@ufrgs.br

Abstract. Rubberlike materials, such as soft biological tissues, may exhibit high nonlinear inelastic responses when subject to large strains. Also, anisotropic inelastic behaviors induced by deformation are observed in the literature. The anisotropic behavior associated with coupled inelastic effects has been a major challenge in the constitutive modeling of materials. Then, this paper presents a variational full-network model capable of representing coupled anisotropic damage and viscoelasticity responses induced by deformation. The proposed model combines the advantages of the full-network and variational frameworks, resulting naturally in a set of scalar minimization problems. The inelastic scalar variables at each material point are related to the quadrature points directions used in the full-network integration scheme, and their evolution is assessed graphically in a very intuitive way. A numerical inflation test of a plate is presented to explore the ability of the proposed model to represent anisotropic damage and viscoelasticity and maintain accuracy for large deformations and increments.

Keywords: viscoelasticity, constitutive modeling, full-network model, variational model, anisotropic damage.

1 Introduction

Materials such as soft biological tissues are considered rubberlike materials. When they are subjected to deformations, nonlinear behaviors may arise. Highly nonlinear responses occur gradually and concomitantly with other complex behaviors. For example, viscous behaviors are easily recognizable by observing creep, relaxation, and hysteresis behaviors. Likewise, in the case of biological tissues, the anisotropic damage behavior presented by these materials can be observed in tissues such as skin, tendons, and arteries when subjected to large deformations since they gradually lose their ability to stretch (Holzapfel [1]). Several works seek to study such mechanical behavior in different loading regimes, compilations of these studies can be found in Humphrey [2], Pena et al. [3], Hamedzadeh et al. [4], which is currently a widely investigated subject.

In order to model and infer the mechanical responses of these materials, different approaches to constitutive modeling of biological tissues have been studied in recent years. A list of these models and their common features are found in Li's work [5]. Generically, such models use hypotheses about the recognized anisotropic characteristics presented by biological tissues. Thus, several models have been developed to represent damage associated with one or more fiber families by Balzani et al. [6], Pena [7], Vassoler et al. [8], or also in fully anisotropic models by Menzel and Waffenschmidt [9] and Saez et al. [10]. A variational framework has been explored to introduce nonlinear inelasticity in isotropic and anisotropic material models, where its main advantage is the flexibility to choose or construct different energy functions to predict the inelastic response. Is has been use for isotropic viscoplasticity [11], anisotropic viscoelasticity [12], and damage and viscoelasticity for fibers [8].

Another relevant and interesting framework to model material, which is capable of dealing naturally with anisotropic elasticity, is the full-network modeling (Menzel and Waffenschmidt [9], Saez et al. [10]). This model consists of the concept of a network of randomly oriented chains at junction points (Wu and Van Der Giessen

[13]). This approach makes it possible to present a completely anisotropic behavior. In recent work, Bresolin and Vassoler [14] unified the variational and full-network frameworks into a variational full network model. Thus, this work aims to study the variational full-network approach by applying it to numerical tests of biological tissues in order to evaluate its capability to represent anisotropic viscosity and damage effects.

2 Variational full-network framework

The variational model is based on the stress calculation through a pseudo-hyperelastic formulation, where the incremental potential Ψ can be determined in order to satisfy eq. (1) (Vassoler et al. [8], Ortiz and Stainier [15].

$$\boldsymbol{S}_{n+1} = 2\frac{\partial \Psi(\boldsymbol{C}_{n+1};\xi_n)}{\partial \boldsymbol{C}_{n+1}} \tag{1}$$

where $\boldsymbol{S}$ is the second Piola-Kirchhoff stress tensor, $\boldsymbol{C}$ is the right Cauchy-Green strain tensor defined by $\boldsymbol{C} = \boldsymbol{F}^T\boldsymbol{F}$, where $\boldsymbol{F}$ is strain gradient. The set ξ corresponds to the state variables of the given problem in terms of $\xi = \xi(\boldsymbol{C}, \lambda^v, \eta)$, where λ^v is a measure of viscous strain, and η is a measure of damage. The subscripts present in the expression eq. (1), n and $n+1$ correspond to the previous and current instants, respectively. In the variational structure, the incremental potential Ψ, takes the form of the expression shown in eq. (2).

$$\Psi(\boldsymbol{C}_{n+1};\xi_n) = \min_{\lambda^v_{n+1},\eta_{n+1}} \{W(\xi_{n+1}) - W(\xi_n) + \Delta t\psi(d^v, \dot{\eta}; \xi_{n+1})\} \tag{2}$$

where the measure $d^v = \dot{\lambda}^v(\lambda^v)^{-1}$. For the deformation measures used, the variable λ^v is obtained from the viscoelastic decomposition of the elongation measure $\lambda = \sqrt{\boldsymbol{m}\cdot\boldsymbol{m}} = \sqrt{\bar{\boldsymbol{F}}\boldsymbol{m}_0\cdot\bar{\boldsymbol{F}}\boldsymbol{m}_0} = \sqrt{\boldsymbol{m}_0\cdot\bar{\boldsymbol{C}}\boldsymbol{m}_0}$, where is defined $\bar{\boldsymbol{F}} = \det(\boldsymbol{F})^{-1/3}\,\boldsymbol{F} = J^{-1/3}\boldsymbol{F}$ with the viscoelastic decomposition shown in eq. (3).

$$\lambda(\bar{\boldsymbol{C}}, \boldsymbol{m}_0) = \lambda^e\lambda^v \quad \boldsymbol{m}_0\cdot\boldsymbol{m}_0 = 1 \tag{3}$$

It is possible to take into account all possible directions that contribute to an elastic energy density φ^e, through the full-network approach (Wu and Van Der Giessen [13]). This determination at a given point in the material is defined by eq. (4).

$$\varphi^e = \int_\Omega C\omega^e d\Omega \tag{4}$$

where C corresponds to the density of the chains as a function of the set of directions Ω and time. Thus $C = C(\Omega(t))$, and Ω corresponds to the set of directions of integration of a point of the material in the current configuration. Rewriting this expression for the reference configuration, and assuming that the orientations of the fibers are random in this reference configuration, the chain density assumes the constant value shown in eq. (5) (Wu and Van der Giessen [16]). Therefore, if evaluated the potential of the previous expression eq.(4), at the current instant eq. (5), is obtained the expression of eq. (6).

$$C\big(\Omega(t=0)\big) = C(\Omega_0) = \frac{1}{4\pi} \tag{5}$$

$$\varphi^e = \frac{1}{4\pi}\int_{\Omega_0}\omega^e d\Omega_0 \tag{6}$$

The integration in eq. (6) for the elastic energy density (φ^e) can be approximated numerically by the algebraic summation of spatial directions resulting in eq. (7). Extending this approach to the viscous (ψ^v) and damage (ψ^η) potentials, and using the same set of orientation vectors and associated weights for each potential, we obtain the expressions eq. (8) and eq. (9), respectively.

$$\varphi^e \approx 2\sum_{k=1}^{m} h_k\omega^e \tag{7}$$

$$\psi^v \approx 2\sum_{k=1}^{m} h_k\omega^v \tag{8}$$

$$\psi^\eta \approx 2\sum_{k=1}^{m} h_k\omega^\eta \tag{9}$$

Equations (7), (8), and (9) correspond to the numerical integration of the presented potentials using the Lebedev quadrature (Govindjee et al. [17]). The potentials ω^e, ψ^v and ψ^η provide flexibility to the model since they can take different forms of expression. Examples of choices for these potentials and how they are treated in variational models can be found in Vassoler et al. [8].

2.1 Incremental solution

For the incremental solution, the rate quantities are considered constant throughout each increment, that is, $d^v \approx \Delta q/\Delta t$ and $\dot{\eta} \approx \Delta\eta/\Delta t$. Thus, the evaluation of the internal variables at t_{n+1} are determined by eq. (10), eq. (11) and eq. (12).

$$\lambda_{n+1}^v = \lambda_n^v \exp(\Delta q) \tag{10}$$

$$\lambda_{n+1}^e = \lambda_{n+1}\lambda_n^{v-1} \exp(-\Delta q) = \lambda^{trial} \exp(-\Delta q) \tag{11}$$

$$\eta_{n+1} = \eta_n + \Delta\eta \tag{12}$$

The potentials W and ψ can be rewritten using the elastic, viscous and damage potentials described, as expressed in eq. (13) and eq. (14).

$$W(\xi) = U(J) + \varphi^e(\lambda^e, \eta) \tag{13}$$

$$\psi\left(\dot{\lambda}^v, \dot{\eta}; \xi\right) = \psi^v(d^v) + \psi^\eta(\dot{\eta}, \eta) \tag{14}$$

where the U potential corresponds to the volumetric potential, φ^e to the elastic potential, ψ^v to the viscous dissipative potential, and ψ^η to the damage dissipative potential.

The minimization presented in eq. (2), can be rewritten using the numerical integration of the potentials φ^e, ψ^v and ψ^η, as shown in eq. (7) to (9). With the "full-network" approach, each fiber orientation has an independent set of variables $\{\lambda_{n+1,k}, \Delta q_k, \Delta\eta_k\}$ that are independent of the set of variables of the other integration orientations. In this case, the system of equations simplifies to one-dimensional problems where the original minimization problem is divided into "m" decoupled minimization problems, eq. (15).

$$2\sum_{k=1}^{m} h_k \min_{\Delta q_k, \Delta\eta_k} \left\{\left(1-\eta_{n+1,k}\right)\bar{\omega}^e\left(\lambda_{n+1,k}^e\right) + \Delta t\left(\omega^v(\Delta q_k/\Delta t) + \omega^\eta\left(\Delta\eta_k/\Delta t; \eta_{n+1,k}\right)\right)\right\} \tag{15}$$

To solve these minimization problems, Newton's method is used. Finally, with the internal variables for each orientation, the stress response to this problem can be determined by eq. (16),

$$\boldsymbol{S}_{n+1} = 2\frac{\partial\Psi}{\partial \boldsymbol{C}_{n+1}} = 2\sum_{k=1}^{m} \frac{\partial\Psi}{\partial\lambda_{n+1,k}} \frac{\partial\lambda_{n+1,k}}{\partial\lambda_{n+1,k}^2} \frac{\partial\bar{\boldsymbol{C}}_{n+1}}{\partial \boldsymbol{C}_{n+1}} : \frac{\partial\lambda_{n+1,k}^2}{\partial\bar{\boldsymbol{C}}_{n+1}} + 2\frac{\partial\Psi}{\partial J_{n+1}} \frac{\partial J_{n+1}}{\partial \boldsymbol{C}_{n+1}} \tag{16}$$

that can be rewritten as eq. (17).

$$\boldsymbol{S}_{n+1} = J_{n+1}^{-\frac{2}{3}} \mathrm{Dev}\left(\sum_{k=1}^{m} \frac{2h_k}{\lambda_{n+1,k}} \frac{\lambda_{n+1,k}^e}{\lambda_{n+1,k}} \frac{\partial\bar{\omega}^e}{\partial\lambda_{n+1,k}^e} \boldsymbol{m}_{0,k} \otimes \boldsymbol{m}_{0,k}\right) + J_{n+1}\frac{\partial U}{\partial J_{n+1}} \boldsymbol{C}_{n+1}^{-1} \tag{17}$$

3 Model application results

To demonstrate the capability of the proposed model, a numerical case of a thin circular plate under cyclic pressure in the z direction was simulated with a pressure rate of $\dot{p} = 100\ Pa/s$. The numerical case is simulated through the finite element method (FEM), using Ansys Mechanical APDL. The eight-node element (SOLID185) was used, which is a general-purpose linear brick element used for the 3D modeling of solid structures. In the eq. (18), eq. (19), eq. (20) and eq. (21) are presented the potentials used in the numerical simulation.

$$\omega = \frac{\mu^*}{\beta^*}\left((\lambda)^{\beta^*} - 1\right) - \mu^*(\lambda - 1) \tag{18}$$

$$\omega^e = \frac{\mu}{\beta}\left((\lambda^e)^{\beta} - 1\right) - \mu(\lambda^e - 1) \tag{19}$$

$$\psi^v = \gamma(d^v)^2 \tag{20}$$

$$\psi^\eta = Y_0 - \delta\log\left(1 - \frac{\eta}{\eta_\infty}\right) \tag{21}$$

where μ^*, β^*, μ, β, γ, Y_0, δ and η_∞ are material parameters presented in Tab. 1. Te rheological representation of this set of potentials is shown in Fig. 1 (Bresolin and Vassoler [14]).

Table 1. Constitutive parameters used in the model

ω	ω^e	ψ^v	ψ^η
$\mu^* = 2 \cdot 10^9$	$\mu = 3 \cdot 10^{11}$	$\gamma = 1.8 \cdot 10^9$	$Y_0 = 0.05$
$\beta^* = 2$	$\beta = 2$	-	$\delta = 7 \cdot 10^8$
-	-	-	$\eta_\infty = 1$

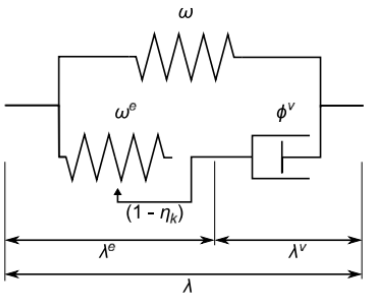

Figure 1. Schematic of the rheological model (Bresolin and Vassoler [14])

The simulated plate has a thickness of 3 mm. For simplicity and to reduce computational efforts, a quarter of the plate was modeled using symmetry boundary conditions. The applied pressure simulating inflation is done with three cycles, with an increasing maximum pressure cycle by cycle, where the maximum peak is 2 kPa, as shown in Fig. 2. The maximum deformed configuration and displacement field can be seen in Fig. 3, where point A (maximum displacement point) is also indicated.

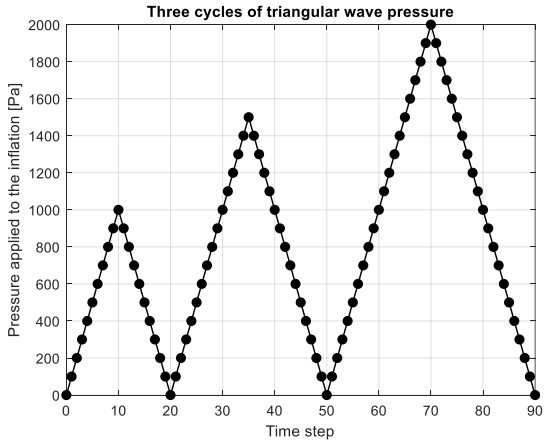

Figure 2. Pressure applied to the plate versus time steps

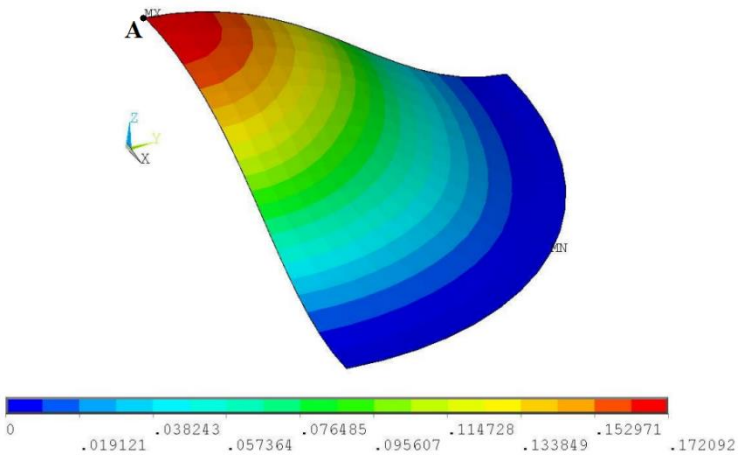

Figure 3. Deformed plate configuration and displacement field

This example has a heterogeneous field response for the quantities. This numerical example investigates point A (see Fig. 3), where the resulting stress-strain curve is presented in Fig. 4, and the history of stress and strain in Fig. 5.

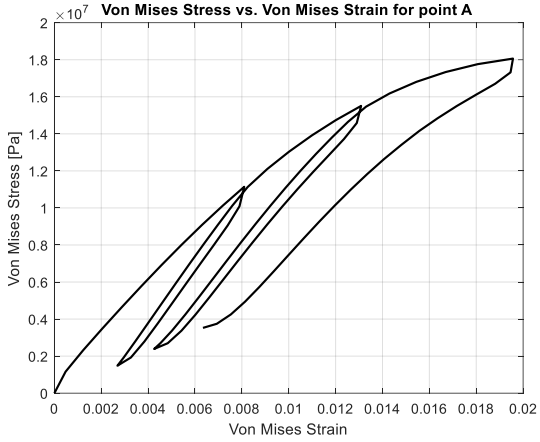

Figure 4. Stress-strain graph at point A

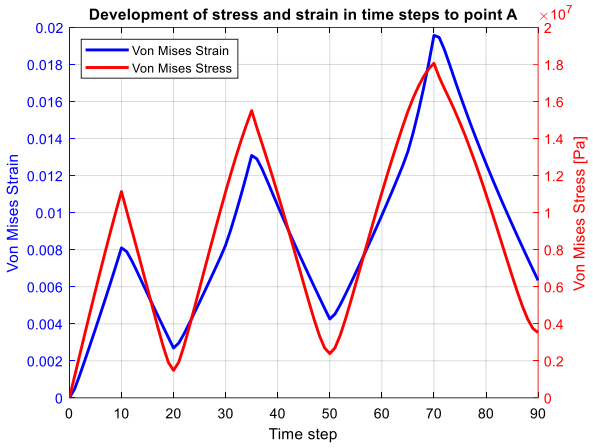

Figure 5. Stress and strain graph for each time step at point A

As observed in the results, the elastic response presents the already expected behavior of non-linearity with viscous effects, evidenced in the evolution of the stress-strain curve during the cyclic loading.

4 Conclusions

In this work, a variational full-network model was studied. The framework incorporates characteristics of variational models to represent characteristic behaviors of soft biological tissues: viscoelasticity, nonlinear behavior, and anisotropic damage. In the constitutive model studied, these behaviors were related to internal variables used for the constitutive model.

The study of the model's ability to simulate biological tissues is still under development. However, the numerical results demonstrate the model's ability to reproduce the inelastic characteristics desired for a pressure load applied to a plate. These results can be used in the future to characterize skin using experimental data obtained from suction experiments such as those performed by [18-20]. Furthermore, as noted in the mathematical

definitions, the model is capable, by simply modifying the potentials, of having its behavior altered, showing flexibility to be able to represent different biological tissues (and other materials with viscoelastic and anisotropic characteristics). For future work, complex geometries and loadings can be explored, in addition to different integration procedures of the variational full-network model.

Acknowledgements. The authors of this work thank CAPES, CNPq and FAPERGS for funding this work.

Authorship statement. The authors hereby confirm that they are the sole liable persons responsible for the authorship of this work, and that all material that has been herein included as part of the present paper is either the property (and authorship) of the authors, or has the permission of the owners to be included here.

References

[1] G. A. Holzapfel, "Similarities between soft biological tissues and rubberlike materials". In: P.-E. Austrell (ed.), *Constitutive Models for Rubber IV*, pp. 607–617. Routledge, 1 edition, 2017.
[2] J. Humphrey, Review Paper: "Continuum biomechanics of soft biological tissues". *Proceedings of the Royal Society of London. Series A: Mathematical, Physical and Engineering Sciences*, vol. 459, n. 2029, pp. 3–46, 2003.
[3] E. Peña, J. A. Peña, and M. Doblaré, "On the Mullins effect and hysteresis of fibered biological materials: A comparison between continuous and discontinuous damage models". *International Journal of Solids and Structures*, vol. 46, n. 7-8, pp. 1727–1735, 2009.
[4] A. Hamedzadeh, T. C. Gasser, and S. Federico, "On the constitutive modelling of recruitment and damage of collagen fibres in soft biological tissues". *European Journal of Mechanics - A/Solids*, vol. 72, pp. 483–496, 2018.
[5] W. Li, "Damage Models for Soft Tissues: A Survey". *Journal of Medical and Biological Engineering*, vol. 36, n. 3, pp. 285–307, 2016.
[6] D. Balzani, J. Schroder, and D. Gross, "A Simple Model for Anisotropic Damage with Applications to Soft Tissues". *Proceedings Applied Mathematics and Mechanics*, vol. 4, n. 1, pp. 236–237, 2004.
[7] E. Peña, "A rate dependent directional damage model for fibred materials: application to soft biological tissues". *Computational Mechanics*, vol. 48, n. 4, pp. 407–420, 2011.
[8] J. M. Vassoler, L. Stainier, and E. A. Fancello, "A variational framework for fiber-reinforced viscoelastic soft tissues including damage". *International Journal for Numerical Methods in Engineering*, vol. 108, n. 8, pp. 865-884, 2016.
[9] A. Menzel, and T. Waffenschmidt, "A microsphere-based remodelling formulation for anisotropic biological tissues". *Philosophical Transactions of the Royal Society A: Mathematical, Physical and Engineering Sciences*, vol. 367, n. 1902, pp. 3499–3523, 2009.
[10] P. Sáez, V. Alastrué, E. Peña, M. Doblaré, and M. A.Martínez, "Anisotropic microspherebased approach to damage in soft fibered tissue". *Biomechanics and Modeling in Mechanobiology*, vol. 11, n. 5, pp. 595–608, 2012.
[11] J. M. Vassoler, E.A. Fancello ; L. Stainier. A Variational Constitutive Update Algorithm For A Set Of Isotropic Hyperelastic¿Viscoplastic Material Models. Computer Methods In Applied Mechanics And Engineering, V. 197, P. 4132-4148, 2008.
[12] J. M. Vassoler; L., Reips; E.A. Fancello. A Variational Framework For Fiber-Reinforced Viscoelastic Soft Tissues. International Journal For Numerical Methods In Engineering, V. 89, P. 1691-1706, 2012.
[13] P. D. Wu and E. Van Der Giessen, "On network descriptions of mechanical and optical properties of rubbers". *Philosophical Magazine A*, vol. 71, n. 5, pp. 1191–1206, 1995.
[14] F. L. Bresolin and J. M. Vassoler, "A variational full-network framework with anisotropic damage and viscoelasticity induced by deformation". *Journal of the Mechanics and Physics of Solids*, vol. 160, n.104777, 2022.
[15] M. Ortiz, and L. Stainier, "The variational formulation of viscoplastic constitutive updates". *Computer Methods in Applied Mechanics and Engineering*, vol. 171, n. 3-4, pp. 419–444, 1999.
[16] P. Wu, and E. Van der Giessen, "On improved network models for rubber elasticity and their applications to orientation hardening in glassy polymers". *Journal of the Mechanics and Physics of Solids*, vol. 41, n. 3, pp. 427–456, 1993.
[17] S. Govindjee, M. J. Zoller, and K. Hackl, "A fully-relaxed variationally-consistent framework for inelastic micro-sphere models: Finite viscoelasticity". *Journal of the Mechanics and Physics of Solids*, vol. 127, pp. 1–19, 2019.
[18] F.M. Hendriks, D. Brokken, C.W.J. Oomens, D.L. Badera, F.P.T. Baaijens , "The relative contributions of different skin layers to the mechanical behavior of human skin in vivo using suction experiments", *Medical Engineering & Physics*, 2006.
[19] B. Muller, J. Elrod, M. Pensalfini, R. Hopf, O. Distler, et al. "A novel ultra-light suction device for mechanical characterization of skin". *PLOS ONE* 13(8), 2018.
[20] B. Mueller, J. Elrod, O. Distler, C. Schiestl, and, E. Mazza "On the Reliability of Suction Measurements for Skin Characterization." *ASME. J Biomech Eng*., 2021.